Formation of Polymerizable Phospholipid Nanotubules and Their Transformation into a Network Gel

Sönke Svenson† and Phillip B. Messersmith*

Division of Biological Materials, Departments of Physical Medicine and Rehabilitation and Biomedical Engineering, Northwestern University, 311 E. Chicago Avenue, Chicago, Illinois 60611

Received December 7, 1998. In Final Form: March 19, 1999

Phospholipids containing diacetylene moieties along their hydrocarbon chains have been extensively studied for their ability to self-assemble into tubule structures from aqueous and aqueous/alcohol solvents. 1,2-Bis(10,12-tricosadiynoyl)-*sn*-glycero-3-phosphocholine ($DC_{8,9}PC$) has previously been shown to form hollow microtubules of length 50−200 μm and average diameter of approximately 0.5 μm. In this paper we report the formation of phospholipid tubules with outer diameters approximately an order of magnitude less than those of pure $DC_{8,9}PC$ microtubules, from a mixture of $DC_{8,9}PC$ and the short chain saturated lipid 1,2-bis(dinonanoyl)-*sn*-glycero-3-phosphocholine (DNPC). Optical and electron microscopy of equimolar aqueous mixtures of $DC_{8,9}PC$ and DNPC revealed the formation of nanotubules of diameter 50−60 nm and length up to 100 μm, after incubation at ambient temperature for several hours. Continued incubation of the nanotubule suspension at ambient temperature caused a gradual transformation of the nanotubules into a lipid gel phase consisting of interconnected helical ribbons. The rate of nanotubule to helical ribbon transformation was lipid concentration dependent; suspensions of higher lipid concentration transformed more rapidly than less concentrated solutions. However, the transformation to helical ribbons could be prevented altogether by storing the nanotubule suspension at 4 °C. Differential scanning calorimetry of the nanotubule and helical ribbon phases revealed endothermic phase transitions at 25.4 and 36.5 °C, respectively. Both phases were polymerized at 10 °C upon exposure to short wave UV (254 nm), as indicated by visible light spectroscopy. NMR analyses suggest that the molecular composition of both phases is close to the expected 1:1 ratio of $DC_{8,9}PC$:DNPC. The nanotubules described herein may have use in technological applications where small diameter, high aspect ratio structures are desired.

Introduction

The study of phospholipid aggregation into robust micro- and nanostructures, such as vesicles, tubules, films, and other structures, is of great importance in understanding phospholipid self-assembly as well as the exploitation of lipid structures for technological use.[1] Of particular interest in this respect are polymerizable phospholipids which contain a diacetylene moiety along their acyl chains; such lipids have been found to self-aggregate into a variety of vesicular and nonvesicular assemblies depending on lipid concentration, structure, and processing conditions.[2−6] The extensively studied 1,2-bis(10,12-tricosadiynoyl)-*sn*-glycero-3-phosphocholine ($DC_{8,9}PC$), so named because it contains eight methylenes between the ester and diacetylene groups, and nine methylenes between the diacetylene and terminal methyl groups (Figure 1), responds strongly to environmental conditions by forming supramolecular structures of different sizes and shapes.[2−6] Predominantly *micro*tubules with a diameter of approximately 0.5 μm and lengths between 50 and 200 μm are formed upon cooling an aqueous suspension of $DC_{8,9}PC$ below the lipid phase transition temperature.[2] Similar microtubules and helical structures are formed upon mixing an ethanolic solution of $DC_{8,9}PC$ with water.[3] Changes in the processing conditions, such as the ratio between alcohol and water, the speed of mixing, the type of alcohol used, and the cooling rate further determine the size and shape of the observed superstructures.[3−6]

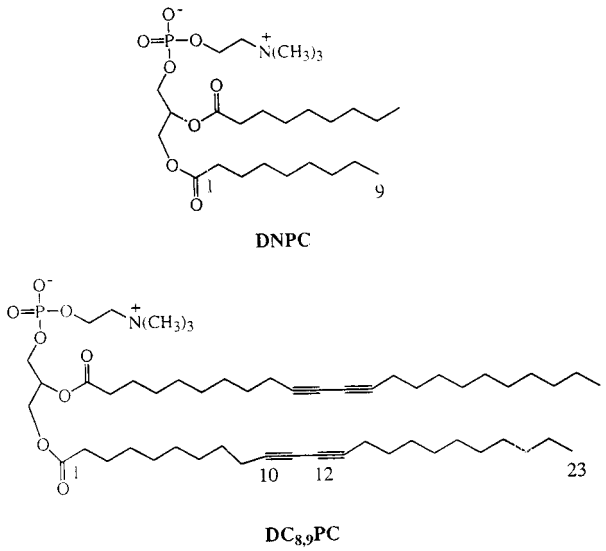

Figure 1. Molecular structures of phospholipids 1,2-bis(10,12-tricosadiynoyl)-*sn*-glycero-3-phosphocholine ($DC_{8,9}PC$) and 1,2-bis(dinonanoyl)-*sn*-glycero-3-phosphocholine (DNPC).

Mixtures of $DC_{8,9}PC$ and other diacetylene-containing lipids with short-chain saturated phosphocholines have been studied to determine the effects of the short-chain

* Corresponding Author: Phone: (312) 503-1789. Fax: (312) 503-2440. E-mail: philm@nwu.edu.

† Present address: Department of Chemical Engineering, Princeton University, Princeton, NJ 08544.

(1) Schnur, J. M. *Science* **1993**, *262*, 1669.
(2) Yager, P.; Schoen, P. E. *Mol. Cryst. Liq. Cryst.* **1984**, *106*, 371.
(3) Georger, J. H.; Singh, A.; Price, R. R.; Schnur, J. M.; Yager, P.; Schoen, P. E. *J. Am. Chem. Soc.* **1987**, *109*, 6169.
(4) Davies, M. A.; Ratna, B. R.; Rudolph, A. S. *Langmuir* **1994**, *10*, 2872.
(5) Spector, M. S.; Selinger, J. V.; Singh, A.; Rodriguez, J. M.; Price, R. R.; Schnur, J. M. *Langmuir* **1998**, *14*, 3493 and references therein.
(6) Thomas, B. N.; Safinya, C. R.; Plano, R. J.; Clark, N. A. *Science* **1995**, *267*, 1635.

10.1021/la981690b CCC: $18.00
Published on Web 05/19/1999

lipids on bilayer structure, aggregate morphology, polymerization of diacetylene lipid, and leakage from mixed lipid vesicles.[7−10] Addition of the short-chain lipid 1,2-bis(dinonanoyl)-*sn*-glycero-3-phosphocholine (DNPC, Figure 1) to $DC_{8,9}PC$ was found to increase polymerization efficiency[7,8] and to alter the size and morphology of aggregates.[7,9] For example, equimolar mixtures of $DC_{8,9}$PC and DNPC were reported to form cylindrical microstructures with diameters ranging from 0.2 to 2.0 μm and lengths ranging from 10 to 70 μm, which gradually reduced in size after 24 h.[9] In a subsequent communication, Markowitz and co-workers reported that the 1:1 mixture of $DC_{8,9}PC$ and DNPC forms a three-dimensional network of interconnected helical threads of width 28 nm upon cooling in water.[10] The structure of the helical threads was unaffected by polymerization, and formed a physical gel at only 0.4 vol % of lipid. Although the authors reported that the superaggregate gel phase formed from preexisting cylindrical structures over a period of several hours, the structure and composition of the cylindrical structures were not fully described.

In this paper we report the results of extensive studies aimed at more fully understanding the nature of both the tubule precursor and network gel phases. Microscopic and calorimetric studies of the 1:1 mixture of $DC_{8,9}PC$ and DNPC revealed the formation of a highly organized *nano*tubule phase which precedes the formation of network gel. The nanotubules have an average diameter of 50−60 nm, were polymerizable, and appear to have a distinctly different structure than conventional $DC_{8,9}PC$ microtubules. The kinetics of nanotubule-to-helical ribbon transformation was found to be dependent on total lipid concentration. NMR spectroscopic analysis indicated that the composition of both nanotubule and network gel phases was close to 1:1 $DC_{8,9}$PC/DNPC.

Experimental Section

1,2-Bis(10,12-tricosadiynoyl)-*sn*-glycero-3-phosphocholine ($DC_{8,9}$PC) and 1,2-bis(dinonanoyl)-*sn*-glycero-3-phosphocholine (DNPC) were purchased as powders from Avanti Polar Lipids, Inc., and used as 12.0 mM stock solutions in chloroform (spectrophotometric grade, Sigma). Water was purified using a Photronix Reagent Grade Water System RGW5 combined with a Photronix Ultrafilter (pH 7.2). In the standard sample preparation protocol, a dried lipid film composed of a 1:1 mixture of $DC_{8,9}PC$ and DNPC was hydrated in ultrapure water at 65 °C and vortexed until a homogeneous suspension was formed. The sample was then allowed to cool to ambient temperature (19−21 °C) and maintained at that temperature for several hours, while 15-μL samples were removed at specified times to study the aggregation and transformation process by transmission electron microscopy.

Transmission electron microscopy (TEM) studies were carried out using a JEOL JEM-1200 EX instrument. The TEM samples were prepared either by transferring 15 μL of the lipid suspension onto a 200 mesh carbon-coated Formvar copper grid (EM Sciences) or by touching one side of the grid onto the gel plug. Excess water was wicked away by touching the edge of the grid with filter paper. Selected samples were then negative stained with 15 μL of 2% (v/w) sodium phosphotungstate at pH 7 for 15 s, after which excess staining reagent was wicked away. Both stained and unstained grids were allowed to dry in air prior to imaging. The morphology of the lipid aggregates was found to be identical for both stained and unstained samples. For optical microscopy, lipid suspensions were imaged at room temperature by placing a drop of the lipid suspension between a glass slide and cover slip. The optical microscope used in this study was a Nikon Eclipse E 600.

Differential scanning calorimetry (DSC) was carried out using a TA Instruments DSC 2920 calorimeter. Lipid suspension (15 μL) was hermetically sealed in an aluminum pan and measured against an empty pan or a pan containing 15 μL of the solvent as reference. The thermograms were recorded at a heating rate of 3 °C/min. Dynamic light scattering was performed on a Coulter N4Plus light scattering instrument at room temperature and a measuring angle of 90°. Suspensions were diluted with Nanopure water just prior to measurement.

Polymerization of the phospholipid suspensions was accomplished by exposure to UV radiation at 254 nm in a Rayonet photochemical reactor. The sample temperature was maintained at 10 °C, to avoid any lipid phase transitions during the irradiation. The exposure times for the nanotubules and helical ribbons were 5, 10, and 20 min. TEM grids of polymerized samples were prepared immediately after irradiation at the same temperature. The UV−vis absorption spectra of lipid suspensions were recorded at 10 °C in a water jacketed 1 × 10 mm quartz cuvette using a Hitachi U 2010 spectrophotometer.

To determine the actual lipid composition (i.e., $DC_{8,9}PC$/DNPC ratio) of the nanotubule and helical ribbon phases, a lipid film of equimolar $DC_{8,9}PC$ and DNPC was hydrated with D_2O as described above to obtain a suspension with total lipid concentration of 12 mM. At this concentration, the formation of nanotubules and their transformation into the helical ribbon (hydrogel) phase at room temperature was slow enough to permit separation and isolation of the two phases for compositional analysis. Immediately after cooling to room temperature, the lipid suspension was separated into two 4-mL portions; one portion was left at 20 °C for 24 h to form the helical ribbon phase while the other was left at 20 °C for 5 h and then refrigerated at 4 °C to retain the nanotubule phase. The nanotubule and helical ribbon suspensions were further subdivided into 2-mL portions of which one each of nanotubules and helical ribbons were polymerized for 20 min at 10 °C as described above. One milliliter of each sample (polymerized nanotubules, unpolymerized nanotubules, polymerized helical ribbons, and unpolymerized helical ribbons) was centrifuged at 14000*g* for 3 min using a Eppendorf Centrifuge 5804R. This permitted a distinct separation between lipid pellet and clear supernatant; the supernatant was then removed by pipet, the residue resuspended in 1 mL of fresh D_2O, and the process repeated. The four washed samples as well as four unwashed control samples were then lyophilized. After lyophilization the samples were each dissolved in 0.5 mL of $CDCl_3$ and analyzed by solution NMR. ^{1}H NMR analyses were carried out on a Varian Gemini 200 spectrometer under standard solution conditions using $\delta(CDCl_3) = 7.26$ ppm as internal standard.

Results and Discussion

The visual appearance of the lipid suspensions was found to be dependent on lipid concentration, temperature, and time. For example, slightly translucent solutions were obtained at very low lipid concentrations (∼0.2 mM) while increasingly turbid suspensions were obtained at ≥3.2 mM. Further increase in lipid concentration resulted in increasingly viscous white suspensions at ≥8.0 mM and viscous white gels which did not flow even after the vials were turned upside down at ≥12.0 mM. Finally, white waxlike solids were formed at high lipid concentrations of ≥34.2 mM. Moreover, every sample became more turbid and viscous during the cooling process and with aging time at ambient temperature. The kinetics of these macroscopic changes were dependent on the lipid concentration. The time required to form a compact hydrogel reduced dramatically with increasing lipid concentration: 20 min at ambient temperature for a 144 mM sample, 15 min for a 192 mM sample, 10 min for a 240 mM sample, and 5 min for a 288 mM sample. It should be noted that physical hydrogel formation was observed at a total lipid concentration of as low as 0.9% (w/v).

(7) Singh, A.; Gaber, B. P. In *Applied Bioactive Polymeric Materials*; Gebelein, C. G., Carraher, C. E., Forster, V. R., Eds.; Plenum: New York, 1988; p 239.

(8) Rhodes, D. G.; Singh, A. *Chem. Phys. Lipids* **1991**, *59*, 215.

(9) Markowitz, M. A.; Chang, E. L.; Singh, A. In *Diagnostic Biosensor Polymers*; Usmani, A. M., Akmal, N., Eds.; ACS Symposium Series 556; American Chemical Society: Washington DC, 1994; p 264.

(10) Markowitz, M. A.; Singh, A.; Chang, E. L. *Biochem. Biophys. Res. Commun.* **1994**, *203*, 296.

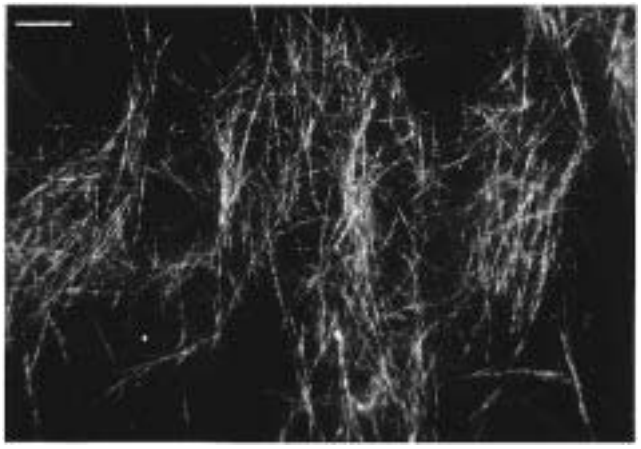

Figure 2. Darkfield optical micrograph of a 1:1 mixture of $DC_{8,9}PC$/DNPC (12.0 mM total lipid concentration) incubated in ultrapure water for 6 h at ambient temperature. Scale bar = 100 μm.

Brightfield, darkfield, and phase contrast optical microscopy of the $DC_{8,9}PC$/DNPC suspensions performed during incubation at room temperature revealed three distinct morphological regimes. Examination of the $DC_{8,9}$-PC/DNPC suspensions immediately after cooling from 65 °C to room temperature revealed the existence of spherical particles (not shown) with an average particle diameter of 827 nm as determined by dynamic light scattering. The spherical particles persisted for several minutes to several hours at room temperature, during which time there was an increase in particle diameter. Gradually there was a transformation from spherical particles to cylindrical structures as shown in Figure 2. The micrograph is dominated by needlelike structures that could best be seen in the dark-field mode. The $DC_{8,9}PC$/DNPC tubules appeared to be of smaller diameter and much less rigid than tubules formed by cooling of an ethanolic solution of pure $DC_{8,9}PC$.[3] Formation of tubules was complete within 5 h of room-temperature incubation of a 6 mM lipid suspension, although the transformation was more rapid at higher lipid concentration. Continued incubation of the tubule suspension at room temperature resulted in the disappearance of tubules and formation of a lipid gel which did not produce defined structures observable under the optical microscope. However, it was found that $DC_{8,9}PC$/DNPC tubules formed at room temperature could be stored indefinitely at 4 °C without any visible change in tubule shape/size, which permitted more detailed examination of the tubule phase by electron microscopy.

TEM micrographs of negative stained samples of the tubule phase in water show nanotubules with uniform diameters between 50 and 60 nm, lengths between 10 and 100 μm, and walls of thickness 8−15 nm (Figure 3). Examination of nanotubules at high magnification revealed that the tubules are composed of a hollow inner core and a wall consisting of two to four lipid bilayers (Figure 3b). Although we can only speculate on the mechanism of nanotubule formation at this time, it is notable that the nanotubules are devoid of the helical markings that are characteristic of pure $DC_{8,9}PC$ microtubules formed in water or aqueous ethanol.[3,11] The helical lines observed on the surface of $DC_{8,9}PC$ microtubules are believed to result from the fusion of curved lipid ribbons

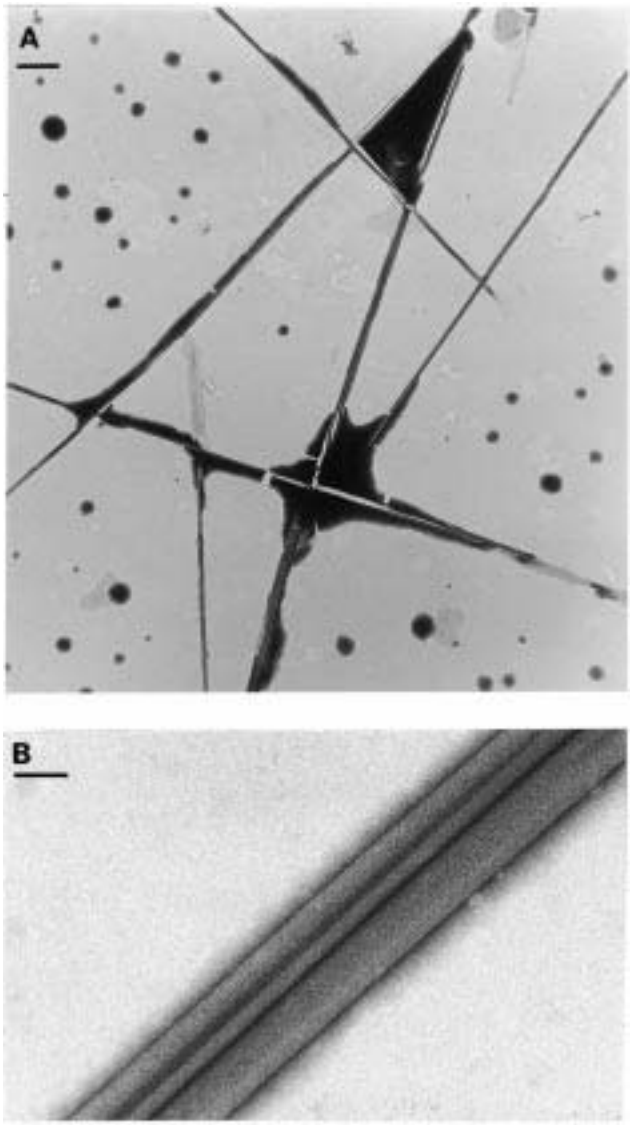

Figure 3. Transmission electron micrographs of a 1:1 mixture of $DC_{8,9}PC$/DNPC (12.0 mM total lipid concentration) after 5 h at ambient temperature: A, low magnification image of nanotubules with outer diameters of 50−60 nm; B, high magnification image of nanotubule wall and the hollow core. The specimen were negative stained using 2% (v/w) sodium phosphotungstate at pH 7. Scale bar = 500 nm (A), 50 nm (B).

that meet edgewise to form the tubules;[12] their absence in the nanotubules may indicate a different mechanism of tubule formation.

TEM examination of $DC_{8,9}PC$/DNPC suspensions incubated for longer periods of time at room temperature indicate that the nanotubules transform into ribbons which radiate in all directions from an entangled core (Figure 4). Helical twisting of the ribbons along their long axis results in the alternating ribbon width observable in the electron micrographs. High magnification images of portions of the ribbons which are oriented parallel to the electron beam direction clearly reveal that the ribbons are two to four lipid bilayers in thickness (Figure 4b). While the lengths of ribbons and nanotubules were virtually identical, the width of the ribbons was found to be 25−30 nm, which is roughly one-half the diameter of nanotubules. The average helix pitch, as measured from the TEM micrographs, was found to approximately 125 nm. The ribbons appear to fuse at contact points with other ribbons within the same particle, as well as with

(11) Ratna, B. R.; Baral-Tosch, S.; Kahn, B.; Rudolph, A. S. *Chem. Phys. Lipids* **1992**, *63*, 47.
(12) Schnur, J. M.; Ratna, B. R.; Selinger, J. V.; Singh, A.; Jyothi, G.; Easwaran, K. R. K. *Science* **1994**, *264*, 945.

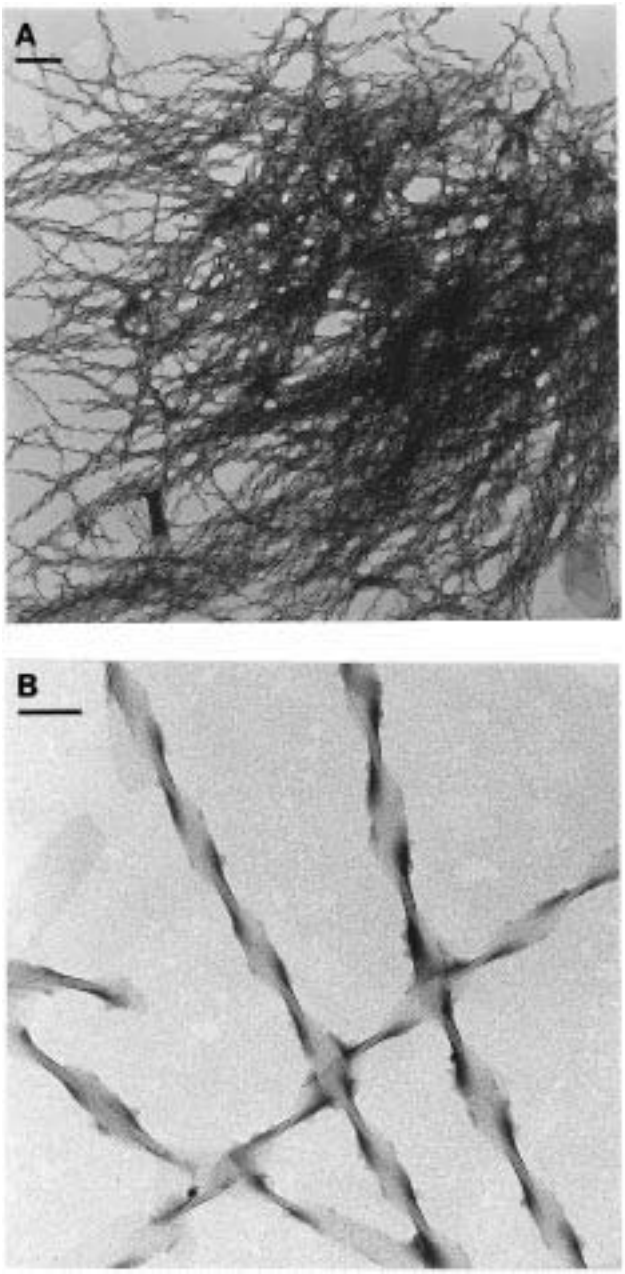

Figure 4. Transmission electron micrographs of a 1:1 mixture of $DC_{8,9}PC$/DNPC (12.0 mM total lipid concentration) after 24 h at ambient temperature: A, low magnification image showing helical ribbon aggregates emanating in all directions from a dense entangled core; B, high magnification image showing the helical nature of ribbons and the apparent fusion of ribbons at junctions. Note the ribbons are of width 25−30 nm and are two to four bilayers in thickness. The specimen were negative stained using 2% (v/w) sodium phosphotungstate at pH 7. Scale bar = 500 nm (A), 50 nm (B).

ribbons emanating from adjacent particles (Figure 4b). Interconnection of helical ribbons to form a three-dimensional network may explain the physical gelation of concentrated lipid suspensions (>0.9% lipid) incubated for several hours at room temperature.[13] The gelation behavior of helical ribbon suspensions is similar to that observed by Markowitz and co-workers.[10]

(13) There were some inconsistencies in the visual appearance of identical samples incubated at room temperature to form the twisted ribbon phase. For example, 12 mM samples sometimes formed a homogeneous gel, while at other times they formed a gel precipitate at the vial bottom with a clear aqueous phase as supernatant. However, the visual appearance of the suspension did *not* affect the microscopic appearance. In both cases electron micrographs revealed virtually identical helical ribbons after 24 h of aging at ambient temperature.

Table 1. Morphological Characteristics of Aggregates Formed by 1:1 Mixtures of $DC_{8,9}PC$/DNPC in Water, as Observed by TEM

lipid concn (mM)	time of incubation at 20 °C[a]					
	2 h	4 h	6 h	18 h	24 h	72 h
0.2				s		
0.6				s		
1.2				s		
2.2	s	s,c	s,c	s,c	s,c,t	s,c,t
2.6	s	s,c	s,c,t		s,c,n	s,c,n,h
3.2	s	s,c	s,c,t	s,c,n	s,c,h	h
4.4	s,c	s,c,t	s,n	s,n	h	h
5.8		s,t,n			h	
8.0		s,n			h	
10.0		s,n			h	
12.0	s,c,t	s,n			h	
14.4		s,n			h	
15.8		n,h			h	
20.0		h			h	
34.2		h			h	
72.0		h			h	
144	h					

[a] Key: s, spherical structures, liposomes; c, clusters of s; t, ill-defined tubules of various lengths and diameters; n, nanotubules; h, helical ribbons. Suspensions were prepared by heating to 65 °C, then cooling to 20 °C, and incubating for specified times.

To reveal more details about the kinetics of nanotubule formation and their transformation into helical ribbons, electron micrographs of a 12.0 mM suspension of $DC_{8,9}PC$ and DNPC were obtained at specific times after cooling to ambient temperature (Figure 5). After incubation for 2 h at ambient temperature, spherical structures, presumably liposomes, and clusters of these aggregates dominate the micrograph. In addition, a few ill-defined tubular structures have been formed within lipid-rich areas (Figure 5a). After 4 h micrographs revealed nanotubules emerging from large tubular structures, which seem to be formed by rolled-up lamellar sheets (Figure 5b). After about 10 h at ambient temperature, nanotubules began to deteriorate and again form lamellar sheets, which appear to be the source for the formation of the helical ribbons (Figure 5c). The nanotubule-to-helical ribbon transformation observed for the 12.0 mM sample was complete within about 18 h at ambient temperature (19−21 °C); however the transformation could be prevented by storing the sample in the refrigerator at 4 °C. For example, nanotubules stored as an aqueous suspension for 3 months at 4 °C appeared identical to freshly prepared nanotubules in electron micrographs (data not shown).

The kinetics of nanotubule formation, as well as nanotubule-to-helical ribbon transformation in water were found to be strongly dependent on the total lipid concentration. Phospholipid suspensions prepared at selected total lipid concentrations between 0.2 and 144 mM were analyzed after 2, 4, 6, 18, 24, and 72 h by TEM to determine the temporal progression of structural development. The results listed in Table 1 reveal that nanotubule formation and transformation to helical ribbons occur faster with increasing total lipid concentration. For example, nanotubules and ribbons were absent at all times when the lipid concentration was below 2.2 mM. The lowest concentration at which nanotubules were detected was 2.6 mM. At a concentration of 15.8 mM, a mixture of nanotubules and ribbons was observed at 4 h instead of the pure nanotubule phase, due to the fast nanotubule-to-helical ribbon transformation. Finally, at a concentration of 144 mM only helical ribbons were observed, even at relatively short incubation times (2 h).

The difference between the two phases formed by 1:1 mixtures of $DC_{8,9}PC$ and DNPC is clearly evident from the DSC thermograms (Figure 6). Heating of an aqueous suspension of nanotubules from 10 to 80 °C produced a sharp endothermic peak at 25.4 °C. The small half-width of the signal reflects the high degree of order within this phase. In contrast, the entangled and interconnected helical ribbons of the hydrogel produce a broad endothermic transition around 36.5 °C, in agreement with the earlier findings of Markowitz and co-workers.[10] Improving the signal-to-noise ratio by increasing the lipid concentration was not successful because this increased the kinetics of nanotubule-to-ribbon transformation (Table 1) and prevented a clear separation of the nanotubule and ribbon phases. A suspension of pure DNPC did not yield an observable phase transition within the 0−50 °C temperature range, whereas a suspension of $DC_{8,9}PC$ exhibited an endothermic chain melting transition at approximately 43 °C (data not shown). The single, lower phase transition temperature observed for the nanotubules and helical ribbons compared to $DC_{8,9}PC$ can be interpreted as formation of a lipid phase containing a mixture of $DC_{8,9}PC$ and DNPC. The difference in observed phase transition temperature between the nanotubules and helical ribbons could reflect either compositional ($DC_{8,9}PC$/DNPC ratio) or structural differences between the two phases.

Exposure of aqueous suspensions of nanotubules and helical ribbons to short-wave UV radiation (254 nm) at 10 °C, a temperature well below the observed phase transitions, resulted in a change of color from white to blue-red. In the case of the nanotubules, the color change was very intense and occurred immediately upon UV irradiation; the color development was more modest and took longer (∼40 s) in the case of the ribbons. UV−vis absorption spectra of the nanotubule and helical ribbon phases polymerized for 5 and 10 min are shown in Figure 7. The nanotubules polymerized for 5 min revealed three distinct maxima, at 499, 533, and 613 nm. Although the 499 and 533 nm bands did not change significantly with increased exposure time, there was an increase in intensity of the 613 nm band with increased irradiation time (Figure 7). The UV−vis spectrum of ribbons polymerized for 5 min was characterized by rather broad maxima around 486 and 521 nm and a sharper peak at approximately 610 nm. There was an increase in the intensity of all peaks with increased UV irradiation of the helical ribbons. The spectra of polymerized nanotubules and helical ribbons closely resemble those previously found for multilamellar vesicular dispersions of $DC_{8,9}PC$ and DNPC at 1:1 and 1:2 molar ratios, respectively.[7] These spectra suggest a high yield of the monomer to polymer conversion, although we currently have no information about the molecular weight of the polymer chains. Polymerization of the diacetylene moieties of $DC_{8,9}PC$ suggests a high degree of order within both nanotubule and helical ribbon superstructures since diacetylene polymerization is known to require structural alignment.[14] We thus conclude that the molecular packing in nanotubules and helical ribbons is similar and provides the required alignment for polymerization. Moreover, the incorporation of a spacer molecule (e.g., DNPC) with the same number of methylene groups is thought to crystallize the proximal and disorder the distal methylene segments of $DC_{8,9}PC$[8] and promote the polymerization of the nanotubule and ribbon superstructures.

DSC measurements of nanotubule suspensions exposed to UV irradiation revealed a dramatic change in the thermograms upon polymerization (Figure 8). The narrow endotherm found for unpolymerized nanotubules at 25.4 °C disappeared completely upon UV irradiation and was replaced by a relatively featureless thermogram. Electron micrographs of the nanotubule phase taken after exposure to UV light for 10 min at 10 °C reveal some significant changes in structure (Figure 9). Polymerization appears to induce destruction of the nanotubules and formation of an interconnected lamellar phase not unlike the

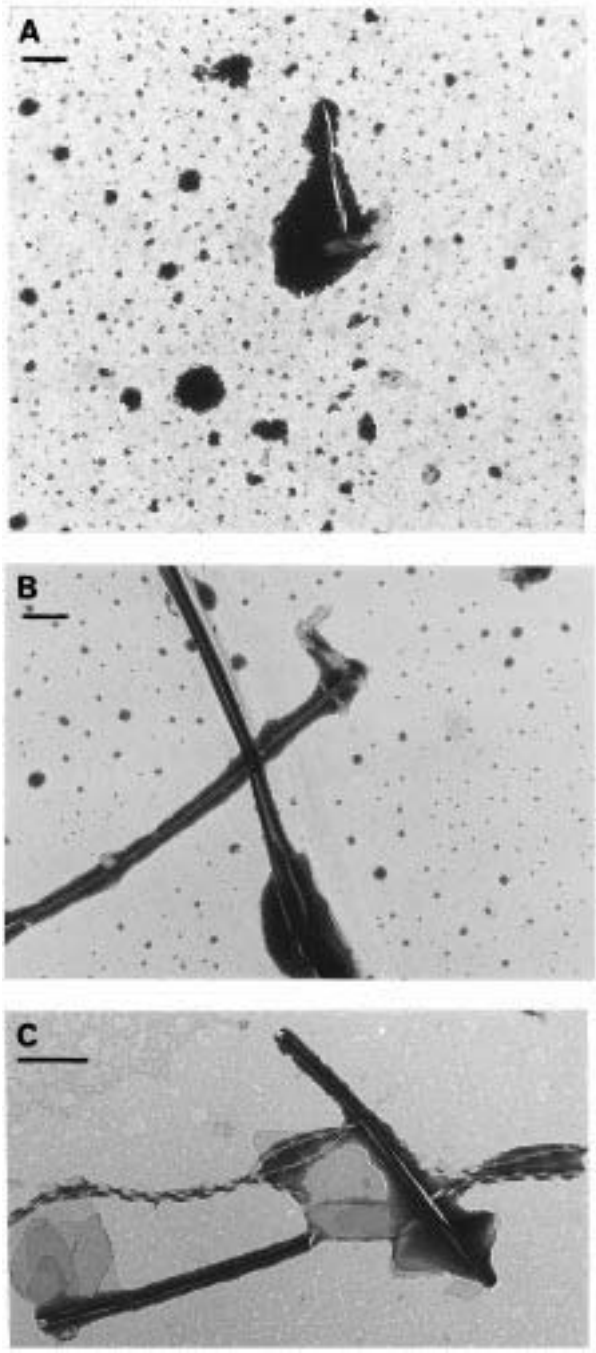

Figure 5. Transmission electron micrographs of nanotubule formation and nanotubule-to-helical ribbon transformation of a 1:1 mixture of $DC_{8,9}PC$/DNPC (12.0 mM total lipid concentration) prepared in ultrapure water, taken after the sample was held for 2, 4, and 10 h at ambient temperature: (A) spherical structures, presumably liposomes, and aggregates of them after 2 h; (B) nanotubule formation from large, ill-defined tubules after 4 h; (C) nanotubule deterioration and helical ribbon formation from lamellar sheets after 10 h. The specimens were negative stained using 2% (v/w) sodium phosphotungstate at pH 7. Scale bar = 500 nm.

(14) Wegner, G. *Makromol. Chem.* **1972**, *154*, 35.

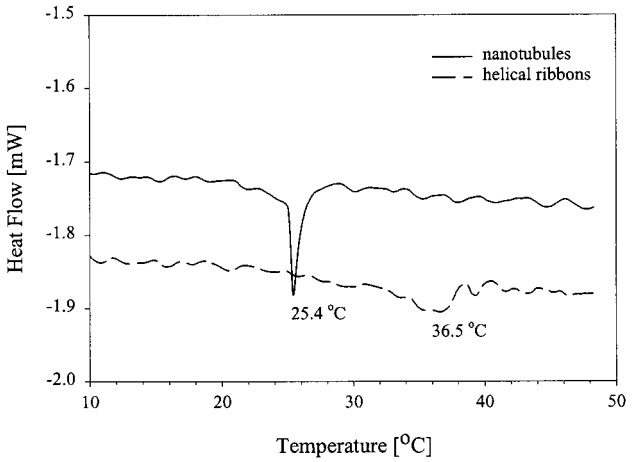

Figure 6. DSC thermograms of aqueous suspensions of nanotubules and helical ribbons prepared from equimolar $DC_{8,9}$-PC/DNPC (12.0 mM total lipid concentration).

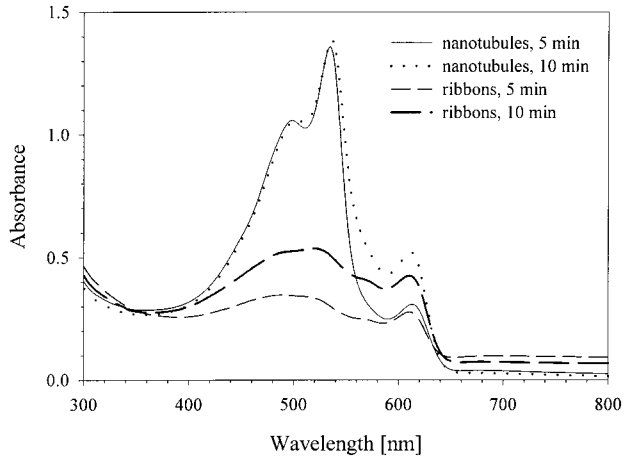

Figure 7. UV−vis absorption spectra of nanotubules and helical ribbons of equimolar $DC_{8,9}$PC/DNPC (12.0 mM total lipid concentration) after UV irradiation at 254 nm for 5 and 10 min at 10 °C. All spectra were recorded at 10 °C.

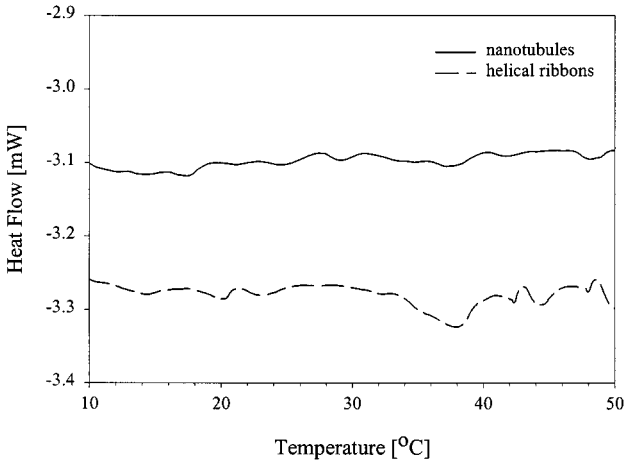

Figure 8. DSC thermograms of aqueous suspensions of nanotubules and helical ribbons prepared from equimolar $DC_{8,9}$-PC/DNPC (12.0 mM total lipid concentration), after UV irradiation at 254 nm for 10 min at 10 °C.

interconnected helical ribbon phase shown in Figure 4. Although some nanotubules remained after polymerization, there was significant damage to their shape, as evidenced by their reduced length and rough surfaces. Furthermore, several of the nanotubule remnants that can be seen in Figure 9 appear to be trough-shaped (i.e., open along one side). These observations suggest a spontaneous nanotubule-to-ribbon transformation triggered by polymerization of $DC_{8,9}$PC. Unfortunately, a quantitative comparison of the thermograms of the helical ribbons before and after UV exposure was not possible. As evident from Figures 6 and 8, the phase transition peaks are rather broad and close to the order of magnitude of the experimental noise. Improving the signal-to-noise ratio by increasing the lipid concentration was impossible because the more rapid nanotubule to helical ribbon

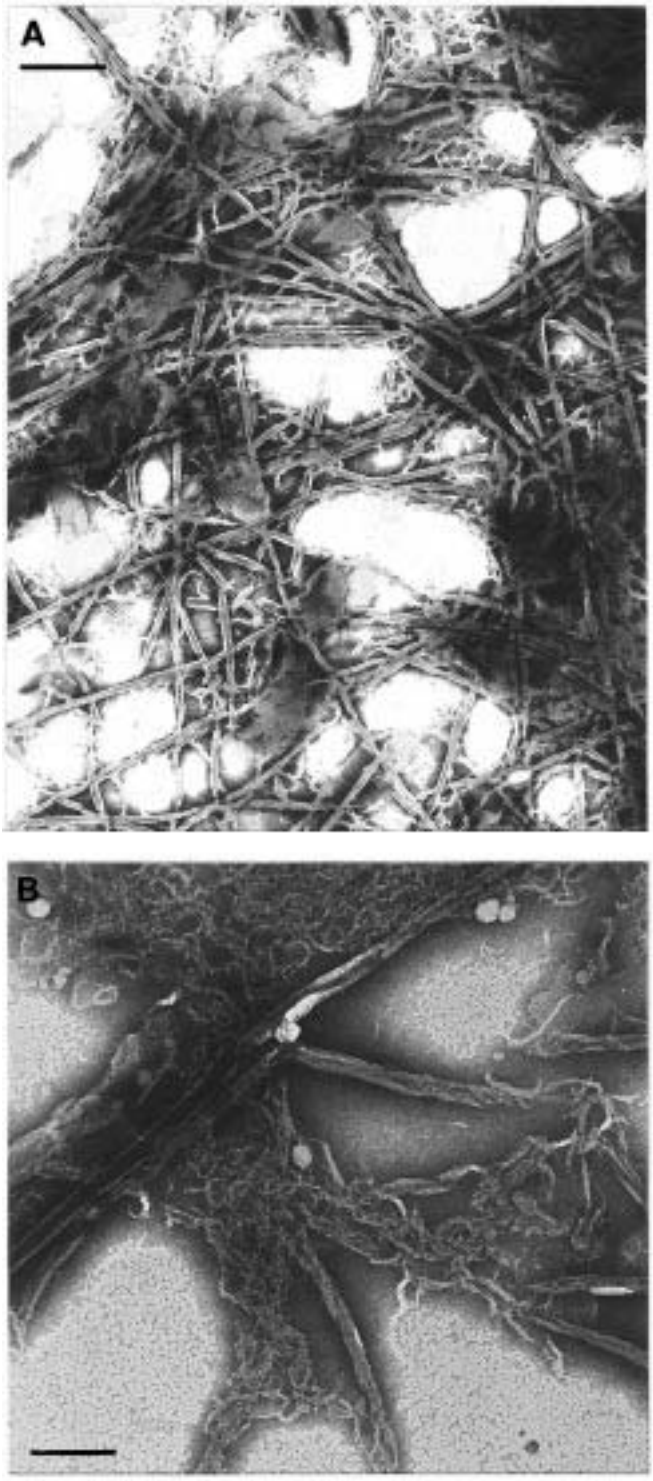

Figure 9. Electron micrographs of the nanotubule phase taken after UV irradiation for 10 min at 10 °C. The specimens were negative stained using 2% (v/w) sodium phosphotungstate at pH 7. Scale bar = 500 nm (A), 200 nm (B).

Table 2. ^{1}H NMR Analysis of Nanotubules and Helical Ribbons[a]

	$CH_2-C\equiv C$	CH_3
expected peak integrals (1:1)	8.0 H	12.0 H
nanotubules, unwashed	8.0 H	12.0 H
nanotubules, washed 2× with water	8.0 H	11.2 H
nanotubules, UV irradiated and unwashed	8.0 H	13.5 H
nanotubules, UV irradiated and washed 2× w/water	8.0 H	10.8 H
helical threads, unwashed	8.0 H	11.2 H
helical threads, washed 2× with water	8.0 H	10.4 H
helical threads, UV irradiated and unwashed	8.0 H	11.6 H
helical threads, UV irradiated and washed 2× w/water	8.0 H	13.4 H

[a] Integrals for multiplets produced by the methylenes in α-position to diacetylene ($CH_2-C\equiv C$) and triplets produced by the terminal methyl groups (CH_3).

tranformation at high lipid concentration prevented a clear separation of the nanotubule and ribbon phases. At this point it remains uncertain whether the peaks above 35 °C in the thermogram of the polymerized ribbons represent phase transitions of polymerized lipid or are experimental noise.

Of significant interest to us is the question of nanotubule and helical ribbon molecular composition. Markowitz and co-workers[10] studied the effect of changes in bulk $DC_{8,9}$PC/DNPC mole ratio on aggregate morphology but did not determine the actual composition of the helical ribbon phase. Although our suspensions were prepared from a lipid film containing a 1:1 mixture of $DC_{8,9}$PC and DNPC, we hypothesized that the actual molecular composition of the aggregates could be quite different since DNPC has a considerably higher solubility in water than $DC_{8,9}$PC,[15] and the concentrations of DNPC used in our studies were above its critical micelle concentration (2.9×10^{-2} mM).[16] We therefore propose two possible nanotubule formation pathways. Both phospholipids could form mixed aggregates with the same 1:1 molar ratio as the lipid film, with DNPC acting as a spacer molecule between $DC_{8,9}$PC monomers as suggested in earlier studies.[7,8,10] Alternatively, DNPC could form micelles which could dissolve $DC_{8,9}$PC monomers and alter the composition of the aggregates. The higher solubility of $DC_{8,9}$PC in this three-component system could result in slower aggregation of the monomers and could influence morphology of the tubules in a similar manner as was found for $DC_{8,9}$PC in alcohol/water mixtures of different compositions.[5] Moreover, it is of interest to determine if the nanotubule-to-ribbon transformation or polymerization alters the composition of the aggregates as well.

To determine the lipid composition of the aggregates, we reasoned that pelletizing the nanotubule and helical ribbon suspensions by centrifugation would permit separation of the aqueous phase from the lipid aggregates. Monomeric and micellar DNPC would remain in the aqueous supernatant phase and could be easily removed by pipet. Redispersal of the lipid aggregates in fresh water and repeating this process would effectively remove the monomeric and micellar DNPC and permit analysis of the composition of the remaining lipid aggregates. This was done by lyophilizing the lipid pellet and dissolving in $CDCl_3$. NMR spectroscopy was then performed on this solution to determine the $DC_{8,9}$PC:DNPC ratio, by comparing the integrated area of the multiplet corresponding to the methylenes in the α-position to the diacetylenes ($DC_{8,9}$PC only) to the integrated area of the triplet corresponding to the terminal methylene groups ($DC_{8,9}$PC and DNPC). A 1:1 mixture of both phospholipids should thus result in an integral ratio of triplet:multiplet of 12:8. The results of the NMR measurements are listed in Table 2. The integral ratio of washed and unwashed nanotubules and helical ribbon samples was close to the expected ratio, indicating that these aggregates have lipid compositions close to 1:1 $DC_{8,9}$PC/DNPC. Furthermore, polymerization did not yield observable changes in lipid composition. The slight deviations observed in some samples did not show an observable trend, and the magnitude of the deviations were within experimental error.

The formation of the nanotubule phase is remarkable for several reasons. Phosphatidylcholines with saturated acyl chains generally form lamellar supramolecular assemblies upon hydration. Introduction of diacetylene groups into the acyl chains has been shown to cause the formation of *micro*tubules of average diameter 0.5 μm,[2−6] and methods used to form $DC_{8,9}$PC tubules generally do not yield much variation in tubule diameter.[3−6] There are several reports of tubule formation from other amphiphiles containing diacetylene groups, but these involve single-chain amphiphiles.[17,18] Diacetylenic hexonamides containing galactonic and mannonic acid headgroups aggregated in water to form tubules with a length of several micrometers and average diameters of 0.3 and 0.4 μm, respectively.[17] The tubules maintained their shape during polymerization, and produced UV−vis spectra similar to the ones we found for the nanotubule phase ($\lambda_{max} = 610$ nm). In samples of the D-galactonamide, right-handed helical structures were found as well.[17] Diacetylenic gluconamides, on the other hand, either formed nanotubules of 50−70 nm in diameter with an aqueous core of 8−10 nm thickness or they aggregated to form micellar rods whose diameter corresponds to a molecular bilayer.[18] It was found that the aggregate formation was dependent on the length of the spacer between the headgroup and the diacetylenes. Nanotubules and micellar rods preserved their morphology upon polymerization except for tubules formed by gluconamides containing only one methylene group as a spacer, which transformed into rods with an approximate diameter of 5 nm, together with a few ribbons.[18] The behavior of this compound upon polymerization resembles in some respects the change in morphology we observed when $DC_{8,9}$PC/DNPC nanotubules were polymerized, although $DC_{8,9}$PC has a much longer spacer between the headgroup and the diacetylene moieties.

The unique properties of phospholipid tubules can be

(15) Although the critical micelle concentration (cmc) of $DC_{8,9}$PC is not known, it is likely to be similar in magnitude to other long-chain phosphatidylcholines such as dipalmitoylphosphatidylcholine, which has a cmc of 4.6×10^{-7} mM (from ref 16).

(16) Marsh, D. *Handbook of Lipid Bilayers*; CRC Press: Boca Rotan, FL, 1990.

(17) Frankel, D. A.; O'Brien, D. F. *J. Am. Chem. Soc.* **1991**, *113*, 7436.

(18) Fuhrhop, J.-H.; Blumtritt, P.; Lehmann, C.; Luger, P. *J. Am. Chem. Soc.* **1991**, *113*, 7437.

(19) Rudolph, A. S. *J. Cell. Biochem.* **1994**, *56*, 183.

exploited for numerous technological uses.[1,19,20] For example, $DC_{8,9}PC$ microtubules have been metalized and incorporated into composites for modification of the electromagnetic properties of materials.[21] $DC_{8,9}PC$ microtubules have also been investigated as controlled-release vehicles for marine[22] (antifouling) and biomedical[23] applications. Although the nanotubules described in this paper have not been investigated in potential applications as yet, the reduction of $DC_{8,9}PC$ tubule diameter into the sub-100 nm range may have an impact on these and other uses for phospholipid tubules. For example, reduction of phospholipid tubule diameter from 0.5 μm to 50 nm is one route to increasing the aspect ratio of metal-clad tubules. Such an increase in tubule aspect ratio could be advantageous from a performance and economic perspective since lower volume fractions of tubules would be required to form a percolation network in a polymer matrix.[24] In the biomedical arena, there are new emerging uses for phospholipid assemblies as biomaterials,[25−27] and the nanotubule to helical ribbon network transformation described herein could be used to form a biocompatible phospholipid-based scaffold for biomedical applications such as drug delivery or tissue engineering.

Conclusions

Equimolar mixtures of the phospholipids $DC_{8,9}PC$ and DNPC suspended in water at 65 °C form a transient nanotubule phase on cooling to ambient temperature. The nanotubule phase was stable for at least 3 months at 4 °C but transforms within hours at ambient temperature into a physical hydrogel consisting of a three-dimensional network of entangled helical ribbons. The kinetics of nanotubule formation and nanotubule-to-helical ribbon transformation depend on the total lipid concentration. Both aggregates consist of the same 1:1 mixture of $DC_{8,9}PC$ and DNPC as the lipid film. Nanotubules and ribbons polymerize during UV irradiation at 254 nm. The nanotubules transform spontaneously into the helical ribbons while the ribbons remain unaltered.

Acknowledgment. The authors thank Professor David Thompson and Marquita Qualls of Purdue University for assistance with light scattering measurements. This work was supported by the National Institutes of Health (Grant DE 12599) and by the Whitaker Foundation. S.S. gratefully acknowledges trainee support by the National Institutes of Health (Grant T32 DE 07042).

LA981690B

(20) Schnur, J. M.; Shashidhar, R. *Adv. Mater.* 1994, *6*, 971.
(21) Schnur, J. M.; et al. *Thin Solid Films* **1987**, *152*, 181.
(22) Price, R.; Patchan, M. *J. Microencapsulation* **1991**, *8*, 301.
(23) Spargo, B. J.; et al. In *Tissue Inducing Biomaterials*; Cima, L., Eyre, R., Eds.; Materials Research Society Symposium Proceedings 252; Elsevier: New York, 1992; pp 285−291.
(24) Stauffer, D.; Aharony, A. *Introduction to Percolation Theory*; Taylor & Francis: London 1994.
(25) Messersmith, P. B.; Vallabhaneni, S.; Nguyen, V. *Chem. Mater.* **1998**, *10*, 109.
(26) Messersmith, P. B.; Starke, S. *Chem. Mater.* **1998**, *10*, 117.
(27) Cui, H.; Messersmith, P. B. In *Tailored Polymeric Materials for Controlled Delivery Systems*; McCulloch, I., Shalaby, S. W., Eds.; ACS Symposium Series 709; American Chemical Society: Washington, DC, 1998; p 203.